

# Neutrinos from stellar core collapses: present status of experiments

O G Ryzhskaya

DOI: 10.1070/PU2006v049n10ABEH006124

## Contents

1. Introduction	1017
2. Neutrino radiation from collapsing stellar cores	1019
3. Methods of neutrino detection in the standard collapse model	1021
4. Identification of a neutrino burst	1021
5. Backgrounds	1021
6. Neutrino detection in the rotating collapsar model	1022
7. Possible interpretation of experimental results obtained during the SN1987A supernova explosion	1022
8. Conclusion: Detectors and observational prospects	1025
References	1027

**Abstract.** The responses of the existing underground detectors to neutrino bursts from collapsing stars evolving in accordance with various models are considered. The interpretation of the results of detecting neutrino radiation from the SN1987A supernova explosion is discussed. A combination of large scintillation counters interlayered with iron slabs (as a target for the electron neutrino interaction) is suggested as a detector for core collapse neutrinos. Bounds for the galactic rate of core collapses based on 28 years of observations by neutrino telescopes of RAS INR, LSD, and LVD detectors are presented.

## 1. Introduction

Neutrinos play an important role in astrophysical research. Neutrinos originate in nuclear reactions deep inside stars but easily leave the star and bear invaluable information on physical process that are hidden from the observer by the thick stellar mantle. The task of experiments in neutrino astrophysics is to obtain this information and to give its correct interpretation.

During the evolution of a massive star (originally composed mostly of hydrogen), the gravitational forces and internal motion of matter in the star result in the formation of the central part (the core) of the star, where the density and temperature are essentially higher than their average values. At some moment, physical conditions favorable for thermonuclear fusion reactions occur in the core. First deuterium and helium are synthesized, then heavier chemical elements are formed: carbon, oxygen, and others up to iron. Heat is

released during the reactions, the core is progressively compressed by gravity at each stage, and the temperature increases. The equilibrium of the star is provided by the balance between gravitational compression and the pressure of the hot gas and radiation. However, after iron nuclei are produced, no heavier elements can be formed, because their synthesis requires expending energy. The gas pressure in the stellar core center cannot equilibrate the gravitational force any more, and gravity starts destroying the iron nuclei. A mixture of protons, neutrons, and electrons with a density  $\sim 10^{14}$  g cm $^{-3}$  is formed. Electrons are squeezed into protons, producing neutrons. Neutronization of the stellar core occurs,



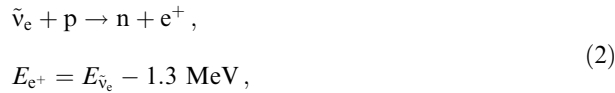
and a short powerful burst of neutrino radiation is produced [1]. The force of gravity rapidly compresses the core and gravitational collapse begins. The collapse can be accompanied by stellar envelope ejection. The optical brightness of the star increases thousands of times over a short time interval, which is manifested as the appearance of a supernova in the sky, which can sometimes be seen even by the naked eye. If the mantle is not ejected or the star is screened by thick interstellar dust clouds, no optical emission can be observed and the detection of neutrino and gravitational radiation is the only way to discover the collapse.

Such, or approximately such, is the possible scenario of the evolution of a star with a mass exceeding 8 solar masses. Theoretical predictions regarding the finale of this scenario depend on the chosen model. Until recently, only spherically symmetric nonrotating stars had been considered. The so-called standard model of the core collapse was elaborated. In this model, the central temperature of a star at the neutronization stage is about  $5 \times 10^{12}$  K, giving rise to 100–200 MeV neutrinos emerging in reaction (1). These neutrinos interact efficiently with matter, scatter, and lose energy, producing the flux of neutrino radiation of all flavors ( $\nu_e, \bar{\nu}_e, \nu_\mu, \bar{\nu}_\mu, \nu_\tau, \bar{\nu}_\tau$ ) with the energy 10–20 MeV, which ultimately escape from the stellar surface. The total energy carried away by the neutrino

O G Ryzhskaya Institute for Nuclear Research,  
Russian Academy of Sciences  
prosp. 60-letiya Oktyabrya 7A, 117312 Moscow, Russian Federation  
Tel. (7-495) 938 57 46, (7-495) 938 19 30  
E-mail: ryzhskaya@lvd.ras.ru; ryzhskaya@vaxmw.tower.ras.ru

Received 22 May 2006, revised 17 July 2006  
*Uspekhi Fizicheskikh Nauk* 176 (10) 1039–1050 (2006)  
Translated by K A Postnov; edited by A M Semikhatov

radiation amounts to 10% of the rest-mass energy of the collapsed stellar core and is shared almost evenly between the six neutrino flavors. The expected duration of the neutrino flux in this process is 5–20 s. The most suitable reaction for search experiments is that of the electron antineutrino interaction with hydrogen:



because this reaction has the maximum cross section.

The experiment is very simple in principle. Detectors filled with a liquid scintillator (scintillation detectors) or with water (Cherenkov detectors) react to positrons produced in reaction (2) and measure their energy. Scintillations produced by positrons are detected by photomultiplier tubes (PMTs). The appearance of a compact series of pulses with the energy 10–20 MeV over a 5–20 s time interval could signal a neutrino burst from a gravitational core collapse [2]. In that case, the number of pulses in the series is proportional to the hydrogen mass in the detector and inversely proportional to the squared distance from the collapsing star.

The main difficulties of the experiment are as follows.

First, the effect can be mimicked by the cosmic ray background. The detectors are therefore set deep underground in galleries or mines and are provided with anti-coincidence systems.

Second, the extremely small interaction cross section of neutrinos with matter and the factor  $1/R^2$  (where  $R$  is the distance to the collapsing star) require hundreds, and better thousands, of tons of hydrogen in the detector equipped with hundreds and thousands of PMTs.

Third, the rate of gravitational collapses in the nearby universe accessible for observations is thought to be around one event every 10–50 years. This fact seems to be the main problem in searches for neutrino bursts from core collapses, because it requires continuous and stable operation of huge multi-channel detectors over dozens of years.

The first detectors to search for core collapse neutrinos were constructed at the Institute for Nuclear Research (INR), the USSR Academy of Sciences: two in the USSR and one in Italy. The elaboration of a liquid scintillator based on white-spirit in 1965 [3] played the decisive role in their construction. This scintillator has outstanding characteristics, including scintillation output, long-term stability, low toxicity, simple manufacturing technology and hence low production costs, and was by far the best on the worldwide market of scintillators. This is also true now, 40 years later.

In 1977, the single-unit ‘Collapse’ detector with the mass 105 tons [4] was installed in a salt mine near Arzamas. In 1978, the multi-unit BUST (Baksan Underground Scintillation Telescope) detector containing 330 tons of scintillator [5] was constructed in a tunnel at the Baksan Neutrino Observatory of INR in the North Caucasus. In 1984, the joint Soviet–Italian multi-unit LSD detector containing 90 tons of scintillator became operational in a tunnel under Mont Blanc (Italy).

In 1986, the Cherenkov detector Kamiokande (KII) containing 2140 tons of water [7] was constructed in Japan. In the same year, the Cherenkov IMB detector with 5000 tons of water [8] started running in the USA.

The possibility of a simultaneous detection of a neutrino burst by several detectors located in different places on the

earth strongly reduces noise and increases the reliability of results.

The ‘moment of truth’ happened on February 23, 1987, when astronomers detected a supernova explosion in a nearby galaxy — the Large Magellanic Cloud, located 50 kiloparsecs away. Later on, this supernova was given the name SN 1987A. Neutrino events connected with this explosion were registered by four neutrino detectors: the LSD, BUST, KII, and IMB (Fig. 1). The ‘Collapse’ detector was not operational on that day. It is seen that the first detection was made by the LSD at 2:52 universal time (UT) [9]. In only about five hours, neutrino signals were registered by the other detectors, the BUST, KII, and IMB. That was puzzling and quite unexpected.

Quite a detailed analysis of the situation with the SN 1987A explosion is performed in paper [10]. Below, we return to some details of that analysis but now we remark on the main point: the results seemed controversial, the standard collapse model clearly did not work.

We note that in the framework of this model, from the very beginning, nobody could obtain the envelop ejection, i.e., the supernova explosion itself [11, 12]. Hopes that this problem would be solved with time have not been fulfilled [13–16]. Therefore, the experimental data on SN 1987A make it especially doubtful that the standard collapse model can be applied in this particular case.

In 1995, the model of the so-called rotational collapsar was finally formulated [17]. This gives the possibility to look quite differently at the final stages of the evolution of a massive star. When rotation is significant, the central part of the star strongly deviates from the spherical shape, becoming reminiscent of a pancake. The central temperature is then two orders of magnitude smaller than in the spherically symmetric model and the energy of electron neutrinos emerging from neutronization is not 100–200 MeV but only 25–55 MeV [18]. The interaction cross section for such low-energy neutrinos with matter is several times lower, and the amount of matter along the line of sight within a broad polar cone is much smaller than in the spherically symmetric model. Therefore, neutrinos travel from the center to the surface of the star almost without interactions and preserve the energy at around 25–55 MeV. In addition, the rotation makes the central part of the star unstable at the neutronization stage: it

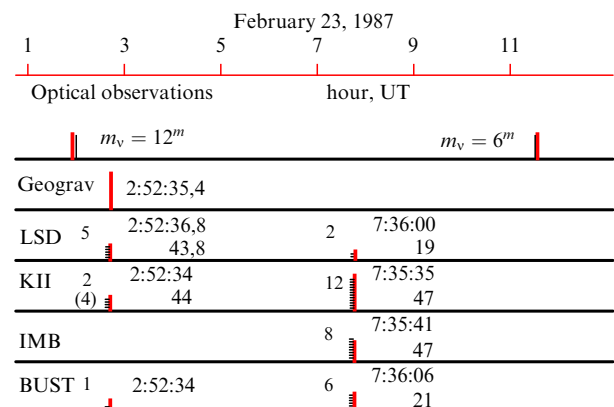


**Figure 1.** Temporal sequence of events observed at different neutrino detectors on February 23, 1987. The number of pulses in the series is conventionally shown for each detector. Times of arrival of the first and last pulse are also indicated.

is disrupted into several pieces, into two smaller stars in the simplest case, which form a close binary system orbiting around the barycenter. In this system, the lighter, less dense star can transfer matter to the heavier, denser one. The duration of this process can be several hours. When the mass of the lighter star has decreased to 0.095 solar masses, the gravitational force can no longer maintain its equilibrium and the star explodes. The observer sees a supernova explosion. The binary system disappears. After that, the second, more massive star collapses, presumably according to the standard model. Thus, the model of gravitational collapse of a rotating star predicts at least two neutrino bursts separated by several hours. The first burst is due to the neutronization of matter in the original rotating stellar core and mainly consists of electron neutrinos  $\nu_e$  with the energy 25–55 MeV. The second burst contains all six types of neutrinos  $\nu_e, \bar{\nu}_e, \nu_\mu, \bar{\nu}_\mu, \nu_\tau, \bar{\nu}_\tau$  with energies 10–20 MeV. The amount of energy in these two neutrino bursts should approximately be in the ratio 1 : 3, and possibly even 1 : 5.

To detect electron neutrinos, reactions of the  $\nu_e$  interactions with nuclei can be used:

$$\nu_e + (A, Z) \rightarrow e^- + (A, Z + 1), \quad (3)$$

$$\nu_e + (A, Z) \rightarrow \nu_e' + (A, Z)^*,$$

where  $A$  and  $Z$  are the atomic number and nuclear charge.

The cross section of reactions (3) depends on the nucleus and the energy of  $\nu_e$ . The largest cross sections are for deuterium, carbon, and heavy nuclei with neutron excess, such as iron or lead.

All hydrogen detectors mentioned above, with the exception of LSD, have a low efficiency in detecting neutrinos with  $E \leq 40$  MeV.

This is because the LSD detector luckily contains, for different reasons (radioactivity shielding, operational security, and, maybe, intuition of the designers of the project), about 200 tons of iron. Thick scintillation counters like LSD provided a sufficiently high detection efficiency of products of the electron neutrino interaction with iron. Estimates show that the first neutrino burst from the collapse is to produce 3–4 pulses at the LSD and only 2–3 pulses at KII, despite the more than 20 times difference in mass in favor of KII [7]. On February 23, 1987, at around 2:52 UT, the LSD detected five pulses.<sup>1</sup> At the same time, only two pulses were detected by the KII detector. In five hours, at about 7:35 UT, the KII detected 12 pulses. At the same time, only one pulse was detected by the LSD, in accordance with the mass difference of the detectors, as indeed it should be for the detection of electron antineutrinos from the second burst associated with the core collapse. Similar reasoning applied to the BUST and IMB shows that they could not ‘see’ the first neutrino burst and ‘saw’ only the second one.

Thus, the picture of events observed on February 23, 1987 can naturally be explained by the rotating collapsar model.

We believe that present searches for stellar core collapse neutrinos should necessarily use detectors containing a sufficient number of heavy nuclei (for example, iron) as a target, in combination with a large amount of liquid scintillator. Cherenkov detectors with deuterium water can also be used. These devices can obtain valuable information

on the dynamics of the gravitational collapse, the temperature, and other parameters of the final stages of stellar evolution.

Finally, we note a possible role of oscillations in generating the neutrino signal reaching the earth. The oscillations can influence the choice of the most effective target material for the detection of neutrinos. The corresponding calculations are to be performed for the most promising nuclei. It is very desirable that future detectors be capable of reliably differentiating between different neutrino flavors. Only under such conditions can one seriously speak about the correspondence of experimental data to various oscillation models. Attempts to use the experimental results from SN 1987A as a touchstone for oscillation models seem to be premature. This is due to uncertainties in the models of the core collapse and neutrino radiation transport through the stellar envelope, in combination with the fairly low statistical significance of the experiment; there are too many free parameters.

## 2. Neutrino radiation from collapsing stellar cores

The elaboration of the rotating collapsar model [17–19] urged the revision of responses of the existing neutrino detectors to a neutrino burst. From the observer’s standpoint, the detection of a neutrino signal in this model must look as follows:

1. There are several neutrino bursts (at least two) separated by the time interval from 400 seconds to eight hours. The first main burst is related to the initial stage of the collapse of the rotating core of a massive star prior to the development of a dynamical instability. This begins under the condition [20, 21]

$$\beta_{\text{cr}} = \frac{\varepsilon_{\text{rot}}}{|\varepsilon_{\text{grav}}|} \geq 0.27,$$

where  $\varepsilon_{\text{rot}}$  and  $|\varepsilon_{\text{grav}}|$  are the total rotational and gravitational energies. The rotational instability leads to fission of the collapsar; in the simplest case, a binary neutron star (NS) system forms. The largest part of the angular momentum of the collapsar  $J_0$  goes into the orbital angular momentum of the binary system  $J_{\text{orb}}$ ,  $J_{\text{orb}} \leq J_0$ . The binary components spiral towards each other due to gravitational wave emission. The time of the coalescence depends on the orbital angular momentum, the collapsar mass  $M_{\text{tot}}$ , and the mass ratio  $\delta = M_1/M_{\text{tot}}$  where  $M_1$  is the mass of the lightest NS [17].

If two equal parts are formed ( $J_{\text{orb}} = 8.8 \times 10^{49}$  erg s<sup>-1</sup> and  $M_{\text{tot}} = 1.8 M_\odot$ , where  $M_\odot$  is the solar mass), the time of coalescence of the components is at the minimum,  $t_{\text{grav}} = 400$  s. In general, the low-mass star begins transferring matter to the more massive one until its mass decreases to the critical value ( $M_{\text{cr}} = 0.095 M_\odot$ ), after which it explodes [22–24]. During the explosion, the iron gas interacts with the iron shell around the neutron star [18], which can also produce an intermediate neutrino burst of a comparably low power. The more massive neutron star collapses according to the standard collapse model, giving rise to the second main neutrino burst. The second main and intermediate neutrino bursts can occur simultaneously or can be separated by a time interval. The time delay between the first and the second bursts is  $400 \text{ s} \leq t_{\text{grav}} \leq 8 \text{ hr}$ .

2. The rotating collapsar is strongly squeezed [18]. Its pole size differs from the equatorial one by several times. The

<sup>1</sup> We stress that such an event took place only once over 15 years of observations from 1984 to 1999 and coincided with the time of the supernova SN 1987 A explosion.

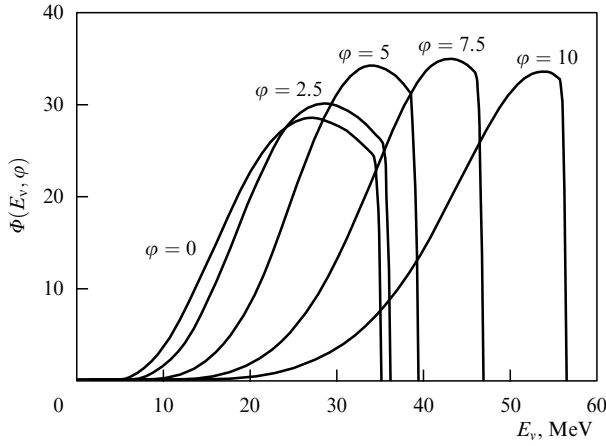
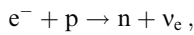


**Figure 2.** The energy neutrino spectrum  $\Phi(E_v, \varphi)$  (in relative units) as a function of the neutrino energy  $E_v$  (MeV) for different  $\varphi$ . The calculation is given for  $\rho_c = 2.6 \times 10^{14} \text{ g cm}^{-3}$ ,  $T_c = 6.2 \times 10^{10} \text{ K}$ ,  $kT_c = 5.34 \text{ MeV}$ ;  $\varphi = \mu_e/kT_c$  is the dimensionless chemical potential of the electron gas;  $\rho_c$  and  $T_c$  are the central density and temperature of the star [18].

instability relative to the azimuthal coordinate at  $\beta = 0.42 > \beta_{\text{cr}}$  [25] rapidly transforms the stellar core into a dumbbell-like configuration with a thin neck. In paper [18], it was therefore suggested that the central part of the rotating collapsar is transparent to the intrinsic neutrino radiation. Because of this, the energy distribution of neutrinos emitted at the first stage of the collapse is then fully determined by the neutronization reaction



in which electron neutrinos with the total energy  $\varepsilon_{\nu_e} = \varepsilon_v = 8.9 \times 10^{52} \text{ erg}$  are generated [18]. The energy spectrum of these neutrinos  $\Phi(E_{\nu_e}, \varphi)$  is rigid and asymmetric, with the mean energy in the range 25–55 MeV (Fig. 2):

$$\Phi(E_{\nu_e}, \varphi) \sim \left( \frac{E_v}{m_e c^2} \right)^5 \frac{1}{1 + \exp(E_v/kT - \varphi)}, \quad (4)$$

where  $\varphi = \mu_e/kT$ , with  $\mu_e$  being the chemical potential of the electrons. The duration of the emission is  $t \sim (2.4-6) \text{ s}$ .

3. The second neutrino burst can be consistent with the ‘standard collapse’ theory, i.e., the theory of nonmagnetized, nonrotating, spherically symmetric stars [26]. This theory implies that the total energy carried away by all neutrino flavors ( $\nu_e, \bar{\nu}_e, \nu_\mu, \bar{\nu}_\mu, \nu_\tau, \bar{\nu}_\tau$ ) is about 0.1 of the rest-mass energy of the stellar core and is approximately equally shared between these six components. The parameters of neutrino fluxes obtained in papers [27–30] (model I) and [31, 32] (model II) are listed in Table 1.

**Table 1.**

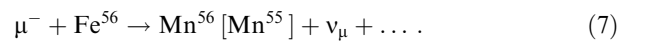
Model	$\varepsilon_1, \text{ erg}$	$\varepsilon_2, \text{ erg}$	$\varepsilon_3, \text{ erg}$	$\bar{E}_{\bar{\nu}_e}, \text{ MeV}$	$\bar{E}_{\nu_e}, \text{ MeV}$	$\bar{E}_{\nu_{\mu,\tau}}, \text{ MeV}$	$T, \text{ s}$
I	$(3-14) \times 10^{53}$	$(0.5-2.3) \times 10^{53}$	$10^{52}$	12.6	10.5	—	20
II				10	8	25	5

*Note.*  $\varepsilon_1$  is the total energy of the explosion carried away by all neutrino species;  $\varepsilon_2$  is the total energy carried away by one neutrino type, where  $\nu_i = \nu_e, \bar{\nu}_e, \nu_\mu, \bar{\nu}_\mu, \nu_\tau, \bar{\nu}_\tau$ ;  $\varepsilon_3$  is the energy carried away by  $\nu_e$  at the neutronization stage over the time interval  $\sim 3 \times 10^{-2} \text{ s}$ ;  $\bar{E}_{\bar{\nu}_e}, \bar{E}_{\nu_e}$ , and  $\bar{E}_{\nu_{\mu,\tau}}$  are spectrum-averaged energies of  $\bar{\nu}_e, \nu_e$ , and  $\nu_{\mu,\tau}$ ;  $T$  is the neutrino burst duration.

We emphasize that the scenario of the final stages of stellar evolution elaborated in the rotating collapsar theory [17, 18] apparently allows more than two (three or more) neutrino bursts.

Indeed, a neutrino outburst can also be initiated by the collision of the expanding gas of iron nuclei (possibly accelerated in the magnetic field) with the iron shell surrounding the inner part of the collapsing core. The kinetic energy per nucleus in such a gas exceeds 300 MeV.

The most plausible value of this energy is 500 MeV. This estimate is obtained by adding the energy of orbital motion (with the velocity 20,000 km s<sup>-1</sup>) and the energy released during the phase transition of the iron-peak rich nuclear gas into neutron matter [19]. At  $E_{\text{Fe}} > 500-600 \text{ MeV}$ ,  $\pi$ -mesons can be generated; they decay to produce neutrinos according to the following scheme:



The neutrino energy spectra thus obtained are fairly rigid with the average values  $E_v \approx 35 \text{ MeV}$  for (5) and (6) and  $E_v \approx 100 \text{ MeV}$  for (7). However, this means of neutrino generation requires further investigation. It is necessary to measure the interaction cross section for the reaction  $\text{Fe} + \text{Fe} \rightarrow \pi^\pm + \dots$  at energies above 300 MeV; it is also necessary to calculate energy spectra of ejected iron nuclei, preferably taking the magnetic field into account.

Measurements of all neutrino flavors over eight hours gives the possibility:

- to detect the collapse event even if the collapse is not accompanied by a supernova explosion;
- to trace the dynamics of the final stage of stellar evolution;
- to estimate the central temperature in the stellar core from the neutrino emission energy;
- to estimate the initial expanding velocity of the iron gas during the stellar explosion (supernova formation);
- to understand the processes leading to the supernova phenomenon;
- to obtain the parameters of the newborn neutron star or arguments in favor of the formation of a black hole as a remnant.

If the collapse proceeds according to the rotating collapsar model, studying the collapse dynamics allows obtaining information on the formation of low-mass neutron stars (lighter than  $0.2 M_\odot$ ).

These light rotating stars result from the initial neutron star disruption. Some of them can escape the gravitational attraction of the more massive counterpart to become

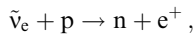
rotating condensation centers for the next generation of stars.

That a neutron star in the center of a normal star can provide sufficient energy and luminosity was suggested by L D Landau about 70 years ago [35]. This idea was abandoned later because the central neutron star in an ordinary star is doomed to rapidly disappear due to the accretion of matter. However, it seems likely now that accounting for the rotation of the central neutron star allows bypassing this difficulty.

It is interesting to note that the existence of a rotating neutron star in the center of the sun could play a certain role in solar energy production in addition to the classical pp and pep cycles and, in principle, be partially responsible for the observed deficit of solar neutrinos.

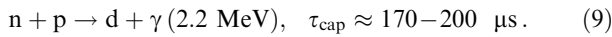
### 3. Methods of neutrino detection in the standard collapse model

So far, Cherenkov ( $\text{H}_2\text{O}$ ) and liquid scintillation ( $\text{C}_n\text{H}_{2n}$ ) detectors that can preferably measure  $\bar{\nu}_e$  have been used to search for and detect core collapse neutrinos. In the ‘standard’ collapse model, the main effect in these detectors is expected from the inverse  $\beta$ -decay reaction:



$$E_{\text{e}^+} = E_{\bar{\nu}_e} - 1.3 \text{ MeV}, \quad \sigma(\bar{\nu}_e \text{p}) \approx 9.3 E_{\text{e}^+}^2 \times 10^{-44} \text{ cm}^2. \quad (8)$$

This reaction is accompanied by neutron capture by hydrogen:



The  $\gamma$ -quantum in (9) can be measured by large scintillator detectors, which helps identify  $\bar{\nu}_e$ . This method was first suggested in paper [36]. Products of reaction (9) can be easily detected against a small background for a high detection efficiency of neutrons  $\eta_n/\bar{N}_b > 1$ , where  $\eta_n$  is the neutron detection efficiency and  $\bar{N}_b$  is the mean number of background pulses in the time interval  $(3\text{--}5)\tau_{\text{cap}}$ .

The  $\nu_e$  scattering reactions have small cross sections, but allow measuring the direction in which neutrinos enter in Cherenkov detectors:

$$\nu_e + \text{e}^- = \nu_e + \text{e}^-, \quad \sigma_{\nu_e \text{e}} = 9.4 E_{\nu_e} \times 10^{-45} \text{ cm}^2, \\ E_{\nu_e} \geq 0.5 \text{ MeV}, \quad (10a)$$

$$\bar{\nu}_e + \text{e}^- = \bar{\nu}_e + \text{e}^-, \quad \sigma_{\bar{\nu}_e \text{e}} = 3.9 E_{\bar{\nu}_e} \times 10^{-45} \text{ cm}^2, \\ E_{\bar{\nu}_e} \geq 0.5 \text{ MeV}, \quad (10b)$$

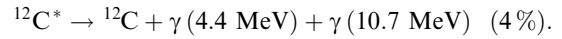
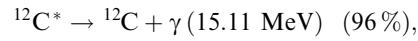
$$\nu_i + \text{e}^- = \nu_i + \text{e}^-, \quad \sigma_{\nu_i \text{e}} = 1.6 E_{\nu_i} \times 10^{-45} \text{ cm}^2, \\ E_{\nu_i} \geq 0.5 \text{ MeV}, \quad (10c)$$

$$\bar{\nu}_i + \text{e}^- = \bar{\nu}_i + \text{e}^-, \quad \sigma_{\bar{\nu}_i \text{e}} = 1.3 E_{\bar{\nu}_i} \times 10^{-45} \text{ cm}^2, \\ E_{\bar{\nu}_i} \geq 0.5 \text{ MeV} \\ (i = \mu, \tau).$$

In liquid scintillation detectors, a neutrino also interacts with carbon. In the ‘standard’ collapse model, the principal reaction is that of level-1<sup>+</sup> (15.11 MeV) excitation in the carbon nucleus via a neutral current:



where  $\nu_i$  is a neutrino of any kind,



The cross section of this reaction is equal to  $\bar{\sigma}_{\nu_e} = 0.066 \times 10^{-42} \text{ cm}^2$  for the Fermi–Dirac neutrino energy spectrum with the mean energy  $\bar{E}_\nu = 10 \text{ MeV}$  (the electron  $\nu_e$  spectrum in the standard model) and  $\bar{\sigma}_{\nu_\mu} = 1.23 \times 10^{-42} \text{ cm}^2$  for the Fermi–Dirac neutrino energy spectrum with the mean energy  $\bar{E}_\nu = 25 \text{ MeV}$  (the muon and  $\tau$  neutrino spectrum in the standard model) [26].

### 4. Identification of a neutrino burst

In the ‘standard’ collapse scenario, the detection of a neutrino burst has the following features:

— a short ( $< 1 \text{ min}$ ) series (clot) of pulses in the energy range 5–50 MeV due to reactions (2), (10), and (11);

— some pulses in the clot must be accompanied by the detection of a  $\gamma$ -quantum at 2.2 MeV from reaction (9) within the time interval  $\sim 1 \text{ ms}$  in the energy range 5 MeV;

— events in the series must be uniformly distributed over the detector volume;

— observation of neutrino bundles by a network of detectors must coincide in time within  $\sim 4 \times 10^{-2} \text{ s}$ . The number of pulses in the series without taking the detector response function into account is

$$N = \frac{1}{4\pi R^2} \sum_{i, r_i} \int_{E_{\text{th}}}^{\infty} I_{\nu_i}(E_{\nu_i}) \sigma_{r_i}(E_{\nu_i}) n_{i, r_i} dE_{\nu_i}, \quad (12)$$

where  $r_i$  is the reaction of the  $\nu_i$  interaction with matter;  $I_{\nu_i}(E_{\nu_i})$  is the energy spectrum of  $\nu_i$ ;  $n_{i, r_i}$  and  $\sigma_{r_i}(E_{\nu_i})$  are the number of nuclei in the target and the  $\nu_i$  interaction cross section for reaction  $r_i$ ;  $E_{\text{th}}$  is the detection threshold; and  $R$  is the distance to the collapsed star.

### 5. Backgrounds

The detector background is a very important characteristic for the registration of neutrino bursts. The count rate of the Poissonian background simulation of a real event is

$$N_k(N_b, T) = N_b \sum_{i=k}^{\infty} \frac{(N_b T)^{i-1}}{(i-1)!} \exp(-N_b T), \quad (13)$$

where  $N_b$  is the count rate of the background pulses,  $T$  is the time interval between the first and  $k$ th pulse in the series, and  $k$  is the number of pulses in the series.

The background is due to:

— cosmic ray muons and secondary particles ( $\text{e}$ ,  $\gamma$ ,  $\text{n}$ ) generated by muons both directly and via nuclear and electromagnetic cascades that develop in the soil and the detector;

— the generation by muons and secondary particles of isotopes with the subsequent decay;

— the natural radioactivity of the surrounding rocks and construction materials ( $\text{e}$ ,  $\gamma$ ,  $\text{n}$ ,  $\alpha$ );

— the natural radioactivity of detectors ( $\text{e}$ ,  $\gamma$ ,  $\text{n}$ ,  $\alpha$ ).

The main source of neutrons in the last two cases is  ${}^{238}\text{U}$  and  ${}^{232}\text{Th}$ . The registration of high-energy neutrons, as well as the simultaneous detection of a photon (electron) and neutron, imitates the detection of an anti-neutrino. To reduce

the background, it is necessary to install the detectors deeply underground, to use low-radioactive materials and active shielding, and to choose a target material that allows reliable identification of events.

The international neutrino detector network (SNEWS), operating in the coincidence mode, helps to significantly relax the background requirements.

## 6. Neutrino detection in the rotating collapsar model

In the rotating collapsar model, electron neutrinos with the spectrum shown in Fig. 2 and the mean energies 25–55 MeV are emitted for 2.4–6 s. Such neutrinos can be detected via the reactions

$$\nu_e + (A, Z) \rightarrow e^- + (A, Z + 1), \quad (14a)$$

$$\nu_e + (A, Z) \rightarrow e^- + (A, Z + 1)^*, \quad (14b)$$

$$\nu_e + (A, Z) \rightarrow \nu_e' + (A, Z)^*. \quad (15)$$

Neutrino interaction cross sections with various nuclei were calculated in papers [37–41]. Figure 3 shows the reduced cross sections of reactions (14a), (14b), and (15),  $\sigma_{\nu_e} = \sigma_{\nu_e A}/N_n$ , as a function of energy for nuclei  $^{12}\text{C}$ ,  $^{16}\text{O}$ , and  $^{56}\text{Fe}$  [37]. It is seen that in the energy range of interest, these cross sections may differ by more than an order of magnitude. For example, at  $E_\nu \leq 40$  MeV,  $\sigma_{\nu_e n}$  for iron exceeds  $\sigma_{\nu_e n}$  for oxygen by more than 20 times.

Cherenkov detectors with  $\text{H}_2\text{O}$ , in which the neutrino interacts with oxygen  $^{16}\text{O}$ , are almost an order of magnitude less sensitive per unit mass than scintillation detectors (which involve carbon  $^{12}\text{C}$ ). These detectors are hardly useful for detecting an electron neutrino with  $E_{\nu_e} \leq 40$  MeV, nor a muon or tau neutrino with  $E_{\nu_{\mu,\tau}} \leq 60$  MeV.

To detect an electron neutrino with energies 20–50 MeV, the most appropriate nuclei are  $^2\text{D}$ ,  $^{56}\text{Fe}$ ,  $^{31}\text{Ga}$ ,  $^{35}\text{Br}$ ,  $^{37}\text{Cl}$ ,  $^{82}\text{Pb}$ . However, not all of them can be used in detectors with the target mass heavier than one kt, some because of their high cost and others due to the complexity of manufacturing the experimental setup.

To detect muon and tau neutrinos, reactions similar to (15) can be utilized.  $^{12}\text{C}$  has a relatively large cross section [41]. Paper [42] suggested using  $^{12}\text{C}$  to search for neutrino oscillations during stellar core collapses.

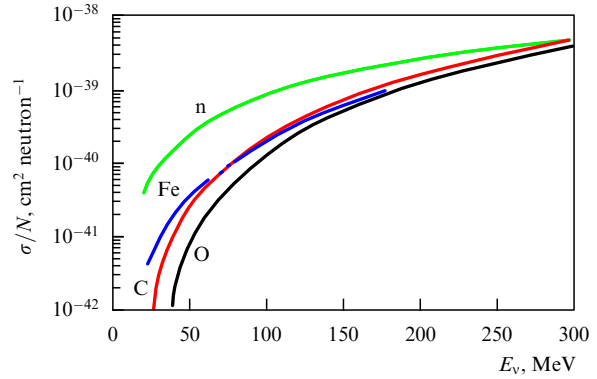


**Figure 3.** The probability of the interaction of electron neutrinos with different nuclei (per neutron) and with free neutrons as a function of the neutrino energy [37].

## 7. Possible interpretation of experimental results obtained during the SN1987A supernova explosion

A supernova explosion was detected in the Large Magellanic Cloud on February 23, 1987. At this time, four underground neutrino detectors were running: two scintillation ones (in the USSR and Italy) and two Cherenkov ones (in the USA and Japan). The parameters of these detectors are listed in Table 2. The effects from reactions (2), (10), and (11) expected in the ‘standard’ collapse model are presented in Table 3. It can be seen that reaction (2) makes the largest contribution to the expected number of events.

To estimate the response of the detectors to the supernova explosion in the rotating collapsar model, we examine the characteristics of these detectors.

The Baksan Underground Scintillation Telescope (BUST) includes 3130 modules [5]. The total mass of the scintillator is 330 tons. The BUST is a 14-meter cube, with two horizontal planes located inside it. Each plane contains 400 scintillation modules  $0.7 \times 0.7 \times 0.3 \text{ m}^3$  in size. Each module-counter is viewed by one PMT with a photocathode diameter of 15 cm (PMT-49B). The distance between the horizontal planes is  $\sim 3.6$  m. Their thickness is  $170 \text{ g cm}^{-2}$  ( $\sim 20 \text{ g cm}^{-2}$  is provided by iron). The scintillator contains white-spirit (the molecular composition is  $\text{C}_n\text{H}_{2n}$ ,  $\bar{n} = 10$ ) [3].

**Table 2.**

Detector	Water equivalent depth	Active material mass (t)	Detection threshold, MeV	Detection efficiency		Background counting rate $N_b \text{ s}^{-1}$ **
				Spectrum $e^+$ reaction $\bar{\nu}_e p \rightarrow e^+ n$ (2)	Spectrum $e^-$ reactions $\nu_e e^- \rightarrow \nu_e e^-$ (10a), (10b) *	
BPST, USSR	850	130 $\text{C}_n\text{H}_{2n}$ 160 Fe	10	0.6	0.15 (0.54)	0.013 (0.033)
LSD, USSR–Italy	5200	90 $\text{C}_n\text{H}_{2n}$ 200 Fe	5–7	0.9	0.4 (0.7)	0.01
KII, Japan–USA	2700	2140 $\text{H}_2\text{O}$	7–14	0.7	0.17 (0.54)	0.022
IMB, USA	1570	5000 $\text{H}_2\text{O}$	20–50	0.1	0.02 (0.18)	$3.5 \times 10^{-6}$

\* Detection efficiencies for electron spectra obtained in reactions  $\nu_{\mu,\tau}(\bar{\nu}_{\mu,\tau}) + e^- \rightarrow \nu_{\mu,\tau}(\bar{\nu}_{\mu,\tau}) + e^-$  (10c) are given in parentheses.

\*\* The background is given in the energy range  $E_{\text{th}} - 50$  MeV; the background for Cherenkov detectors is given for the detection of internal events.

**Table 3.**

Detector	$K_{e^+}(2)$	$K_{e^-}(10a)+(10b)$	$K_{e^-}(10c)$
LSD	1.5	0.043	0.024
BUST	2	0.052	0.036
KII	17	0.53	0.36
IMB	6	0.4	0.35

The detection energy threshold is  $\sim 10$  MeV. The active volume of the telescope that is used to search for core collapse neutrinos comprises counters collected in three horizontal planes: two inner planes and one bottom plane. The mass of the scintillator amounts to 132 tons. In analyzing the results obtained on February 23, 1987, the authors also used information provided by some external detectors. This allowed them to increase the working mass to 200 tons.

The LSD detector [6], which was operating under Mont-Blanc at the depth 5200 m.w.e., consisted of 72 scintillation counters (Fig. 4) joined in nine modules allocated at three levels (three modules in each) with the area  $6.4 \times 7.4$  m<sup>2</sup>. The height of the LSD is 4.5 m. Each module consisted of an iron container with the area  $6.4 \times 2.14$  m<sup>2</sup> and height 1.5 m, with the wall thickness 2 cm. The module's interior was separated into eight cells by iron slabs 2 cm thick. Scintillation counters  $1 \times 1 \times 1.5$  m<sup>3</sup> in size were set in the cells. Each counter was watched by three PMTs with the photocathode diameter 15 cm (PMT-49B). The high sensitivity and low background of the detector allowed measurements of both a positron and a neutron generated in reaction (2) via their capture by hydrogen (9). The capture time in the scintillator was  $\tau \sim 170$   $\mu$ s. Gamma-quanta ( $E_\gamma = 2.2$  MeV) were detected in a time window (with the energy threshold 0.8 MeV) that opened for 500  $\mu$ s after each pulse with an energy above 5 MeV. The efficiency of neutron detection by the same counter that measured positrons was  $\sim 50\%$ . With the possibility of the detection of gamma-quanta by neighboring counters taken into account, the neutron detection efficiency increases to 80%.

The Cherenkov detector Kamiokande II (KII) [7] consisted of two coaxial cylinders. The external cylinder was 19.6 m in diameter and 22.5 m in height; the diameter and height of the internal cylinder were 15.6 m and 16 m, respectively. The detector was filled with water. The mean absorption length of Cherenkov light was 45 m. The detector

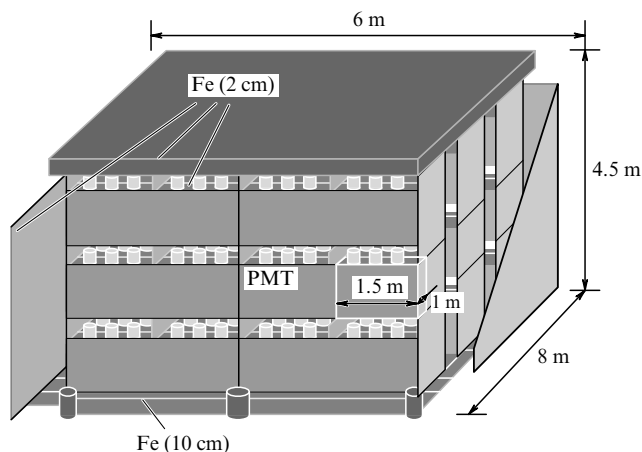


**Figure 4.** Liquid scintillation detector LSD; PMT — photo-multiplying tube.

was viewed with 900 photomultipliers with the photocathode diameter 50 cm allocated over the surface of the internal cylinder which contained 2140 tons of water. The efficiency of detection of pulses depended on the energy threshold and was 50% for  $E = 8.5$  MeV and 90% for  $E = 14$  MeV.

The large Cherenkov detector IMB (Irvine–Michigan–Brookhaven) [8] consisted of a rectangular parallelepiped  $22.5 \times 17 \times 18$  m<sup>3</sup> in size, filled with water. The active volume of 5000 m<sup>3</sup> was viewed with 2048 PMTs with the photocathode diameter 20 cm allocated over six planes of the detector. The detection efficiency of pulses in IMB was 14% for the energy  $E = 20$  MeV, 56% for  $E = 30$  MeV, and 89% for  $E = 50$  MeV.

Figure 1 shows the time sequence of events observed on February 23, 1987 at different detectors. It can be seen that the events are grouped at two moments: at 2:52:36 UT, when the main signal was detected in the LSD, and at 7:35:35 UT, when significant signals were obtained at KII and IMB.

We examine the LSD events in more detail. The parameters of pulses detected at 2:52 UT and 7:35 UT are presented in Table 4. The third column of the table shows the energy of the pulses corresponding to two energy calibrations carried out by measuring the spectrum of energy losses of cosmic ray muons before and after February 23, 1987 (each calibration spanned three months). The accuracy of the energy measurement is  $\sim 20$ –25%. We note that the LSD detected a series of five pulses in real time before information on the SN 1987A explosion was received. The probability of a pure coincidence in the registration of such an event with the supernova explosion is less than  $10^{-3}$  per year [9]. Such a series had not been registered since the beginning of operation of the LSD, both from 1984 to 1987 and from 1987 to 1999. It is true, however, that the detector background was reduced in 1988 due to additional shielding. Thus, we conclude that the LSD event is significant.

At 2:52:35.4 UT, pulses were also registered by two gravitational wave antennae (in Rome and Maryland) [43]. Strong correlations between pulses in the gravitational wave antennae and in neutrino underground detectors were observed on February 23 from 2:00 UT to 8:00 UT [44, 45].

Events detected by the IMB, KII, and BUST at 7:35 UT were analyzed after the information on the supernova explosion had been obtained. These events were interpreted by the majority of physicists as the observation of the antineutrino flux from SN 1987A.

Attempts to explain the LSD event in the same way met with certain difficulties.

- First of all, at 2:52 UT, the KII measured 2 or 4 pulses [46],<sup>2</sup> i.e., the LSD detected more pulses than the KII.

**Table 4.**

Event No.	Time, UT $\pm 2$ ms	Energy, MeV
1	2:52:36.79	7–6.2
2	40.65	8–5.8
3	41.01	11–7.8
4	42.70	7–7.0
5	43.80	9–6.8
1	7:36:00.54	8
2	7:36:18.88	9

<sup>2</sup> The number of pulses depends on the accuracy of the correspondence of the timescale used to the universal time.

Assuming that both detectors measured antineutrinos, such a relation could be possible only if the collapsar emitted low-energy antineutrinos (we recall that the LSD energy threshold is 5 MeV, while that of KII is more than 7 MeV). But such an assumption requires the total energy carried away by neutrinos from the collapsar to be  $E_\nu = 6E_{\bar{\nu}} \approx 1.2 \times 10^{55}$  erg [10]. This energy is more than an order of magnitude higher than the binding energy of a neutron star with the mass  $\sim 2 M_\odot$ .

• Second, of the five pulses detected by the LSD, only one was accompanied by a small photon pulse with the energy  $\sim 1.4$  MeV, which appeared 278 mcs after the trigger. On average, assuming the detection of antineutrinos, two to three pulses should be accompanied by the detection of a 2.2 MeV photon due to neutron capture (9). The probability that only one neutron is detected under these conditions is less than 5%.

Therefore, the explanation of the LSD effect in terms of the detection of antineutrinos appears unlikely. All attempts to explain the contradictory results obtained on February 23, 1987 using the standard collapse model have failed. However, after the model that took the rotation of the star into account had been suggested, the results obtained 19 years ago could be reconsidered. The explanation of the LSD effect by the rotating collapsar model seems quite natural. We recall that the first neutrino burst in that model mainly consists of electron neutrinos. With neutrino oscillations taken into account, all types of neutrinos (but not antineutrinos) with  $E_\nu \leq 60$  MeV can reach Earth [18].

The observation of electron neutrinos can be done via reactions (14a) and (14b) and the observation of muon and tau neutrinos via some reaction similar to (15). For simplicity, we first consider the interaction of an electron neutrino with nuclei present in the above detectors.

The IMB and KII contained oxygen, mostly  $^{16}\text{O}$ ; the LSD and BUST contained carbon  $^{12}\text{C}$  and iron. The LSD contained 200 tons of  $^{56}\text{Fe}$ , the BUST 160 tons of  $^{56}\text{Fe}$ . As follows from [37], at  $E_{\nu_e} \leq 40$  MeV, the interaction cross section  $\sigma_{\nu_e n} = \sigma_{\nu_e A}/N_n$  (where  $N_n$  is the number of neutrons in the nucleus) exceeds  $\sigma_{\nu_e n}$  for oxygen by more than 20 times. Thus, the number of  $(\nu_e, ^{56}\text{Fe})$  interactions in the 200 tons of iron in the LSD is higher than that of  $(\nu_e, ^{16}\text{O})$  interactions in 1900 tons of oxygen (2140 tons of  $\text{H}_2\text{O}$ ) in the KII. In the case of the neutrino interaction with iron via neutral currents, the cross section ratio is even higher for iron [37, 38, 40].

We consider in more detail how  $(\nu_e, \text{Fe})$  interactions could be detected in the LSD. Table 5 lists partial cross sections for the reaction



at  $E_{\nu_e} = 40$  MeV [39].

The ground level is  $0^+$  for iron  $^{56}\text{Fe}$  and  $4^+$  for cobalt  $^{56}\text{Co}$ . The difference in the binding energy between these nuclei is  $E[{}^{56}_{27}\text{Co}] - E[{}^{56}_{26}\text{Fe}] = 4.056$  MeV.

The energy threshold for reaction (16) is 8.16 MeV. The electron is born with an energy from 33.7 to 24.7 MeV, and its appearance is always accompanied by the cascade  $\gamma$ -quanta with the total energy from 1.72 to 10.7 MeV. We recall that the critical energy ( $\epsilon$ ) in iron (the energy at which ionization losses are equal to radiation losses) is 21 MeV. Therefore, an electron with energy  $E \geq \epsilon$  traveling in an iron slab of thickness  $d > 1$  units (where  $t$  is the radiation length unit,

**Table 5.**

1) GT* $\sigma = 5.36 \times 10^{-41}$ cm <sup>2</sup>	$E_{K,e^-}^{***} = 33.7$ MeV, $\sum_n E_\gamma = 1.72$ MeV
2) F** $\sigma = 1.29 \times 10^{-40}$ cm <sup>2</sup>	$E_{K,e^-} = 31.84$ MeV, $E_\gamma = 1.88$ MeV, $n\gamma: \sum_n E_\gamma = 1.72$ MeV
3) GT $\sigma = 1.27 \times 10^{-41}$ cm <sup>2</sup>	$E_{K,e^-} = 28.2$ MeV, $E_\gamma = 3.6$ MeV, $E_\gamma = 1.88$ MeV, $n\gamma: \sum_n E_\gamma = 1.72$ MeV
4) GT $\sigma = 7.1 \times 10^{-41}$ cm <sup>2</sup>	$E_{K,e^-} = 27.2$ MeV, $E_\gamma = 4.6$ MeV, $E_\gamma = 1.88$ MeV, $n\gamma: \sum_n E_\gamma = 1.72$ MeV
5) GT $\sigma = 1.48 \times 10^{-40}$ cm <sup>2</sup>	$E_{K,e^-} = 24.7$ MeV, $E_\gamma = 7.1$ MeV, $E_\gamma = 1.88$ MeV, $n\gamma: \sum_n E_\gamma = 1.72$ MeV

\* Gamow–Teller resonance

\*\* Fermi level

\*\*\* Kinetic energy of the electron

1  $t$ -unit = 13.9 g cm<sup>-2</sup>, i.e., 1.78 cm for iron) should produce a small electromagnetic cascade. Calculations show that when neutrinos with the energy  $E_{\nu_e} = 40$  MeV interact with iron nuclei in a target of thickness 2–3 cm, located between two scintillation layers, more  $\gamma$ -quanta than electrons enter the scintillator [18, 47, 48]. The mean energy of these particles is 7–9 MeV. The detection efficiency of the  $(\nu_e, \text{Fe})$  interaction ( $\eta_{\nu_e}$ ) depends on the construction of the detector and on the energy threshold. The detection efficiency averaged over volume is  $\bar{\eta} = 45$ –50% for the LSD and  $\bar{\eta} \leq 15\%$  for the BUST. Figure 5 shows the expected energy spectra from pulses in the LSD produced by neutrinos with  $E_{\nu_e} = 40$  MeV [48]. It can be seen that the mean energies, which should have been detected by the LSD in the scenario under consideration, correspond to the ones actually measured by this detector on February 23, 1987.

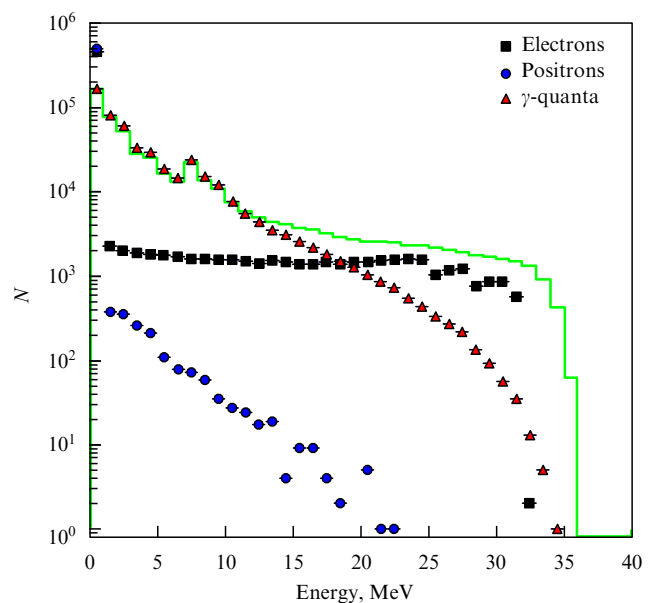


**Figure 5.** The energy loss spectrum of products of reaction (16) in the scintillator [48] ( $N$  is the number of events).



Table 6.

Detector	Detection threshold	Estimate of the number of $\nu_e A$ interactions				Estimate of the effect	Experiment
		$N_1$	$N_2$	$N_3$	$N_4$		
LSD	5–7	3.2	5.7	3.5	4.9	3.2	5
KII	7–14	0.9	3.1	1.2	2.5	2.7	2*
BPST	10	2.8	5.2			$\sim 1$	1**

\* See [46]  
\*\* See [34]

Estimates of neutrino radiation detection during the first phase of the collapse of a rotating star are presented in Table 6. Cross sections for the reactions ( $\nu_e, {}^{56}\text{Fe}$ ), ( $\nu_e, {}^{12}\text{C}$ ), and ( $\nu_e, {}^{16}\text{O}$ ) are taken from papers [37, 39–41]. The estimates are made for monochromatic neutrinos with  $E=30$  MeV ( $N_1$ ) and  $E=40$  MeV ( $N_2$ ), as well as for spectrum (4) at  $\varphi=5$  ( $N_3$ ) and  $\varphi=7.5$  ( $N_4$ ).

It is seen that these estimates obtained in the rotating collapsar model are consistent with experimental data.

Thus, the entire ensemble of pulses detected by the LSD, KII, IMB, and BUST on February 23, 1987 from 2:52 UT to 7:35 UT is in good agreement with the predictions of the rotating collapsar model.

Here, we also note that the remnant of the supernova explosion SN 1987A displays an asymmetric quasi-ellipsoidal form, strongly elongated in one direction (Fig. 6).

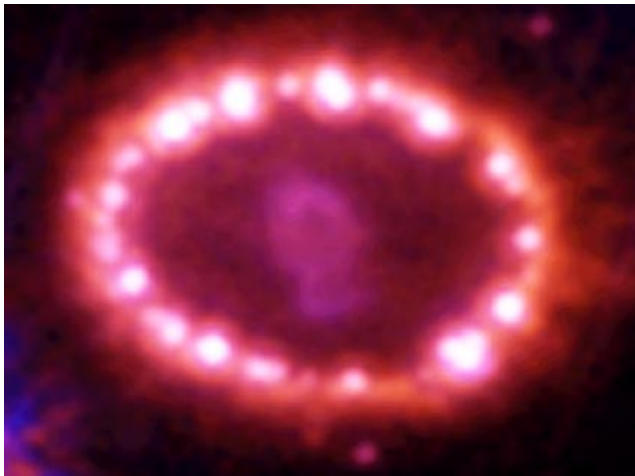


**Figure 6.** On February 1987, light from the brightest stellar explosion observed in recent times, SN 1987A, arrived at the earth. This picture, taken by the Advanced Camera for Survey on board the Hubble Space Telescope in November 2003, shows the site of the explosion 16 years later. The picture shows that the shock wave from the explosion continues to impact with the gaseous ring that existed prior to the explosion, and the supernova remnant at the center continues to expand. Hot bright spots, reminiscent of pearls in a cosmic collier, emerged in the middle of the 1990s when the shock heated the gas up to several million kelvins. Since then, astronomers have been watching the gaseous ring in all spectral bands. The supernova SN 1987A is located in the Large Magellanic Cloud — a nearby galaxy 170 thousand light years away. This means that the explosion itself — the collapse and detonation of a star about 20 times as massive as the sun — occurred 170 thousand years before February 1987. (The picture is taken from The Hubble Heritage Information Center: <http://heritage.stsci.edu>. Credit to P Challis, R Kirshner (CfA), and B Sugerman (STScI), NASA).

## 8. Conclusion: Detectors and observational prospects

Unfortunately, stellar core collapses are very rare events. Over the last thousand years, written sources reported on only five supernova explosions in our galaxy. So-called ‘hidden’ collapses are possible, however, which occur without the envelope ejection or are enshrouded by dust. Theory predicts that the galactic rate of such collapses is around one per 20 years. It is therefore necessary to use detectors capable of observing the core collapse neutrino bursts expected in different collapse scenarios. The devices must operate continuously over many years and, in order not to run idle, be multi-purpose.

Presently, a number of large detectors, which are used in various fields of underground physics (neutrino physics, cosmic ray physics, searches for rare events predicted by theory), are operating: Super-Kamiokande (SuperK), KamiLAND, SNO, and LVD. The parameters of these installations are listed in Table 7 and their location is shown in Fig. 7. The mass of the active material used in the SNO (heavy water), LVD and Kam LAND (scintillator) is around one kt; in the SuperK (pure water), it amounts to 22.5 kt. In addition, there are two scintillation detectors with smaller masses: the ASD (Artemovsk, Ukraine, INR RAS) — 0.1 kt and the BUST (Baksan, Russia, INR RAS) — 0.2 kt. Despite relatively small volumes, these devices, which have been running for more than 27 years, are capable of detecting neutrino radiation from stellar core collapses in our galaxy and are used to watch for the collapses.

Table 7 shows the expected effects produced in different detectors from a stellar collapse in the center of the galaxy in both the standard scenario and the rotational collapsar model (from the first neutrino burst with the mean neutrino energies 30 and 40 MeV). It is seen that the maximum number of interactions in the first case should be observed by the SuperK due to the large mass of the detector. In the second case, at  $E_\nu \sim 40$  MeV, the effect in the LVD and SNO detectors is comparable with that in the SuperK, and at  $E_\nu < 30$  MeV, it should exceed the number of events in the SuperK due to the small neutrino interaction cross section with oxygen.

We emphasize that the Russian–Italian LVD detector located at the underground Gran Sasso Laboratory of the National Institute for Nuclear Physics of Italy (INFN) has been searching for core collapse neutrinos since 1991. It contains  $\sim 1$  kt of scintillator and  $\sim 1$  kt of iron. The LVD is capable of detecting not only  $\bar{\nu}_e$  but also  $\nu_e$ . Over 14 years of observation, no gravitational collapses have been discovered in the galaxy or Magellanic Clouds, including hidden ones (without envelope ejection). The upper bound for the rate of core collapses in these galaxies at a 90% confidence level is

Table 7.

Detector	Depth, m.w.e.	Mass, kt	Threshold, MeV	Efficiency			Expected number of events					Background, $s^{-1}$
				$\eta_{e^+}$	$\eta_n$	$\eta_\gamma$	Standard model [1]		Rotating collapsar model			
							$\tilde{\nu}_e p$ ( $\tilde{\nu}_e D + \nu_e D$ )	$\nu_i e^-$	$\nu_i C$	$\nu_e A$	$\nu_e C$	
Arteomovsk ASD, Russia	570	0.105 $C_n H_{2n}$	5	0.97	0.8	0.85	57	2.1	9.5		19* 9**	0.16
Baksan BPST, Russia	850	0.13 (0.2) $C_n H_{2n}$	10	0.6		0.2	45 (67)	1.4 (2.2)	2.8 (4.3)		5* (8) 3** (4)	0.013 (0.033)
KamLAND, USA – Japan	2700	1 $C_n H_{2n}$	$\sim 4$	0.9			500	22	85		180* 80**	
Gran Sasso LVD, Italy – Russia	3300	0.95 Fe 1 $C_n H_{2n}$	4–6	0.9	0.6	0.55	500	22	55	250* 100**	110* 50**	< 0.1
Kamioka SuperK, Japan – USA	2700	22.5 $H_2O$	5.5	0.9			9400	400		650* < 160**		
SNO, Canada	6000	1 $D_2O$	5				700	16		600* 350**		

\* Number of events for  $E_{\nu_e} = 40$  MeV

\*\* Number of events for  $E_{\nu_e} = 30$  MeV

less than one event per six years. With the data from the Collapse detector (Arteomovsk, 1977), BUST (1978), LSD (1984–1999), and LVD (1991) taken into account, the upper bound for the rate of core collapses in the galaxy is below one event per 12 years at a 90% confidence level.

The LVD, SuperK, and SNO belong to the global network for searches for neutrino bursts from collapsing stars (SNEWS), which has been running since 2001.

To conclude, we all wish supernova explosions occurred more frequently and closer (but not too close) to the earth.

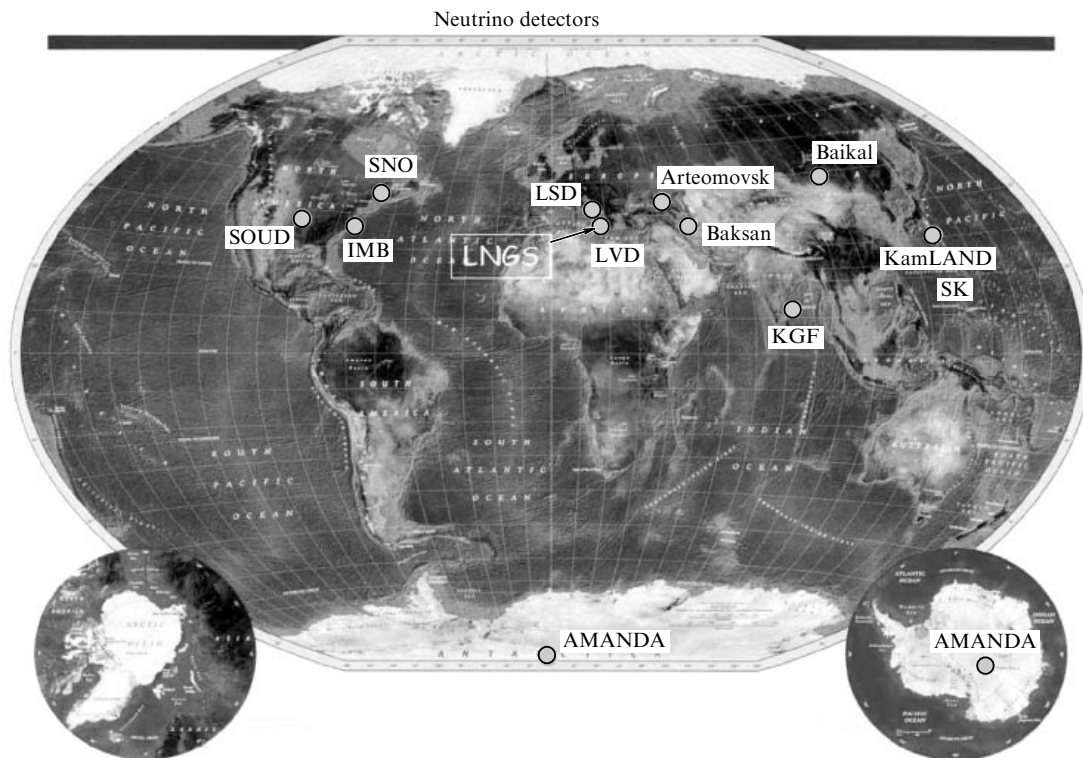


Figure 7. Locations of the existing and currently running neutrino detectors.

## References

1. Zel'dovich Ya B, Guseinov O Kh *Dokl. Akad. Nauk SSSR* **162** 791 (1965)
2. Domogatsky G V, Zatsepin G T, in *Proc. of the 9th Intern. Conf. on Cosmic Rays, London, UK, 1965* Vol. 2 (Ed. A C Stickland) (London: The Institute of Physics and The Physical Society, 1965) p. 1030
3. Voevodskii A V, Dadykin V A, Ryazhskaya O G *Prib. Tekh. Eksp.* (1) 85 (1970)
4. Korchagin P V et al., in *Proc. of the 16th Intern. Cosmic Ray Conf., Kyoto, Japan, 1979* Vol. 10 (Ed. S Miyake) (Tokyo: Institute for Cosmic Ray Research, Univ. of Tokyo Press, 1979) p. 299
5. Alekseev E N et al., in *Proc. of the 16th Intern. Cosmic Ray Conf., Kyoto, Japan, 1979* Vol. 10 (Ed. S Miyake) (Tokyo: Institute for Cosmic Ray Research, Univ. of Tokyo Press, 1979) p. 282; in *Proc. of the 12th Intern. Conf. on Neutrino Physics and Astrophysics, Sendai, Japan, 1986* (Eds T Kitagaki, H Yuta) (Singapore: World Scientific Publ. Co., 1986) p. 270
6. Badino G et al. *Nuovo Cimento C* **7** 573 (1984); Dadykin V L et al., in *Proc. of the 16th Intern. Cosmic Ray Conf., Kyoto, Japan, 1979* Vol. 10 (Ed. S Miyake) (Tokyo: Institute for Cosmic Ray Research, Univ. of Tokyo Press, 1979) p. 285
7. Hirata K et al. *Phys. Rev. Lett.* **58** 1490 (1987)
8. Bionta R M et al. *Phys. Rev. Lett.* **58** 1494 (1987)
9. *IAU Circ.* (4316) (1987); *IAU Circ.* (4323) (1987)
10. Dadykin V L, Zatsepin G T, Ryazhskaya O G *Usp. Fiz. Nauk* **158** 139 (1989) [*Sov. Phys. Usp.* **32** 459 (1989)]
11. Nadyozhin D K *Astrophys. Space Sci.* **49** 399; **51** 283 (1977); **53** 131 (1978)
12. Bruenn S W *Phys. Rev. Lett.* **59** 938 (1987)
13. Herant M, Benz W, Colgate S *Astrophys. J.* **395** 642 (1992)
14. Janka H-T, Müller E *Astron. Astrophys.* **290** 496 (1994)
15. Burrows A, Hayes J, Fryxell B A *Astrophys. J.* **450** 830 (1995)
16. Imshennik V S, Litvinova I Yu *Yad. Fiz.* **69** 660 (2006) [*Phys. At. Nucl.* **69** 636 (2006)]
17. Imshennik V S *Space Sci. Rev.* **74** 325 (1995)
18. Imshennik V S, Ryazhskaya O G *Pis'ma Astron. Zh.* **30** 17 (2004) [*Astron. Lett.* **30** 14 (2004)]
19. Aksenov A G et al. *Pis'ma Astron. Zh.* **23** 779 (1997) [*Astron. Lett.* **23** 677 (1997)]
20. Tassoul J-L *Theory of Rotating Stars* (Princeton, NJ: Princeton Univ. Press, 1978)
21. Lai Dong, Shapiro S L *Astrophys. J.* **442** 259 (1995)
22. Blinnikov S I et al. *Astron. Zh.* **67** 1181 (1990) [*Sov. Astron.* **34** 595 (1990)]
23. Imshennik V S *Pis'ma Astron. Zh.* **18** 489 (1992) [*Sov. Astron. Lett.* **18** 494 (1992)]
24. Aksenov A G, Blinnikov S I, Imshennik V S *Astron. Zh.* **72** 717 (1995) [*Astron. Rep.* **39** 638 (1995)]
25. Imshennik V S, Nadyozhin D K *Pis'ma Astron. Zh.* **18** 195 (1992) [*Sov. Astron. Lett.* **18** 79 (1992)]
26. Imshennik V S, Nadyozhin D K *Usp. Fiz. Nauk* **156** 561 (1988) [Translated into English: in *Soviet Scientific Reviews (1988–1989)* (Ser. E: Astrophys. and Space Phys., Vol. 7) (Chur: Harwood Acad. Publ., 1989) p. 75]
27. Arnett W D *Can. J. Phys.* **44** 2553 (1966)
28. Ivanova L N et al., in *Trudy Mezhdunarodnogo Seminara po Fizike Neitrino i Neitrinnoi Astrofizike* (Proc. Intern. Seminar on Physics of Neutrino and Neutrino Astrophysics) Vol. 2 (Moscow: FIAN SSSR, 1969) p. 180
29. Imshennik V S, Nadyozhin D K, in *Itogi Nauki I Tekhniki* (Advances in Science and Technology) (Ser. "Astronomiya" (Astronomy), Vol. 21 (Moscow: VINITI AN SSSR, 1982) p. 63
30. Nadezhin D K, Otroshchenko N V *Astron. Zh.* **57** 78 (1980) [*Sov. Astron.* **24** 47 (1980)]
31. Bowers R, Wilson J R *Astrophys. J.* **263** 366 (1982)
32. Wilson J R et al. *Ann. N.Y. Acad. Sci.* **470** 267 (1986)
33. Aglietta M et al. *Europhys. Lett.* **3** 1315 (1987); Dadykin V L et al. *Pis'ma Astron. Zh.* **14** 107 (1988) [*Sov. Astron. Lett.* **14** 44 (1988)]
34. Alekseev E N et al. *Pis'ma Zh. Eksp. Theor. Fiz.* **45** 461 (1987) [*JETP Lett.* **45** 589 (1987)]
35. Landau L D *Dokl. Akad. Nauk SSSR* **17** 301 (1937); *Nature* **141** 333 (1938)
36. Chudakov A E, Ryajskaya O G, Zatsepin G T, in *Proc. of the 13th Intern. Conf. Cosmic Ray, ICCR, Denver, CO, USA, 17–30 August, 1973* Vol. 3 (Ed. R L Chasson) (Boulder, CO: Univ. of Denver, Colorado Associated Univ. Press, 1973) p. 2007
37. Bugaev E V et al. *Nucl. Phys. A* **324** 350 (1979)
38. Kolbe E, Langanke K, Krewald S *Phys. Rev. C* **49** 1122 (1994); Kolbe E, Langanke K *Phys. Rev. C* **63** 025802 (2001)
39. Gaponov Yu V, Ryazhskaya O G, Semenov S V *Yad. Fiz.* **67** 1993 (2004) [*Phys. At. Nucl.* **67** 1969 (2004)]
40. Haxton W C *Phys. Rev. D* **36** 2283 (1987)
41. Fukugita M, Kohyama Y, Kubodera K *Phys. Lett. B* **212** 139 (1988)
42. Ryazhskaya O G, Ryasny V G, Saavedra O *Pis'ma Zh. Eksp. Theor. Fiz.* **59** 297 (1994) [*JETP Lett.* **59** 315 (1994)]
43. Amaldi E et al. *Europhys. Lett.* **3** 1325 (1987)
44. Pizzella G *Nuovo Cimento B* **102** 471 (1989)
45. Aglietta M et al. *Nuovo Cimento C* **12** 75 (1989)
46. De Rújula A, in *Proc. EPS, Conf., Uppsala, 1987; Phys. Lett. B* **193** 514 (1987)
47. Dedenko L G, Fedunin E Yu, private communication (2003)
48. Boyarkina V V, Master Thesis (Moscow: Moscow Institute of Physics and Technology, State Univ., 2004)